Neurobiology of Disease 127 (2019) 312–322

Contents lists available at ScienceDirect

Neurobiology of Disease

journal homepage: www.elsevier.com/locate/ynbdi

Nucleolin reorganization and nucleolar stress in Purkinje cells of mutant *PCD* mice

Fernando C. Baltanás[a,1], María T. Berciano[b,1], Olga Tapia[b], Josep Oriol Narcis[b], Vanesa Lafarga[c], David Díaz[d], Eduardo Weruaga[d], Eugenio Santos[a], Miguel Lafarga[b,*]

[a] Lab.1, CIC-IBMCC (Universidad de Salamanca-CSIC) and CIBERONC, Salamanca, Spain
[b] Department of Anat and Cell Biology and "Centro de Investigación Biomédica en Red sobre Enfermedades Neurodegenerativas (CIBERNED)", University of Cantabria-IDIVAL, Santander, Spain
[c] Laboratory of Genomic Instability, "Centro Nacional de Investigaciones Oncológicas" (CNIO), Madrid, Spain
[d] Laboratory of Neural Plasticity and Neurorepair, Institute for Neuroscience of Castilla y León, Universidad de Salamanca, Salamanca, Spain.

ARTICLE INFO

Keywords:
Agtpbp1
CCP1
Neurodegeneration
Nucleolar stress
Nucleolin
Purkinje cells

ABSTRACT

The Purkinje cell (PC) degeneration (*pcd*) mouse harbors a mutation in *Agtpbp1* gene that encodes for the cytosolic carboxypeptidase, CCP1. The mutation causes degeneration and death of PCs during the postnatal life, resulting in clinical and pathological manifestation of cerebellar ataxia. Monogenic biallelic damaging variants in the *Agtpbp1* gene cause infantile-onset neurodegeneration and cerebellar atrophy, linking loss of functional CCP1 with human neurodegeneration. Although CCP1 plays a key role in the regulation of tubulin stabilization, its loss of function in PCs leads to a severe nuclear phenotype with heterochromatinization and accumulation of DNA damage. Therefore, the *pcd* mice provides a useful neuronal model to investigate nuclear mechanisms involved in neurodegeneration, particularly the nucleolar stress. In this study, we demonstrated that the *Agtpbp1* gene mutation induces a p53-dependent nucleolar stress response in PCs, which is characterized by nucleolar fragmentation, nucleoplasmic and cytoplasmic mislocalization of nucleolin, and dysfunction of both pre-rRNA processing and mRNA translation. RT-qPCR analysis revealed reduction of mature 18S rRNA, with a parallel increase of its intermediate 18S-5'-ETS precursor, that correlates with a reduced expression of *Fbl* mRNA, which encodes an essential factor for rRNA processing. Moreover, nucleolar alterations were accompanied by a reduction of PTEN mRNA and protein levels, which appears to be related to the chromosome instability and accumulation of DNA damage in degenerating PCs.

Our results highlight the essential contribution of nucleolar stress to PC degeneration and also underscore the nucleoplasmic mislocalization of nucleolin as a potential indicator of neurodegenerative processes.

1. Introduction

The Purkinje cell degeneration (*pcd*) mutant mouse harbors a mutation in the *Agtpbp1* gene, also known as *Nna1* gene (Fernandez-Gonzalez et al., 2002). This gene encodes for the cytosolic carboxypeptidase protein (CCP1), which is essential for the stabilization of microtubules (Kalinina et al., 2007; Muñoz-Castañeda et al., 2018; Zhou et al., 2018). In this vein, a recent study indicates that CCP1 also regulates mitochondrial mobility and fusion through deglutamylation of tubulin (Gilmore-Hall et al., 2018).

Interestingly, the *pcd* mutation induces a different primary postnatal degeneration of the several neuronal populations (Blanks et al., 1982; Fernandez-Gonzalez et al., 2002; Greer and Shepherd, 1982; O'Gorman and Sidman, 1985), making this animal model highly appropriate for studying different kinds of degenerative processes in neurons affected by the same mutation. In this regard, while degeneration of photoreceptors takes about 1 year (Blanks et al., 1982), and the death of the thalamic neurons and the mitral cells occurs at 6 and 4 months of age, respectively (O'Gorman and Sidman, 1985; Valero et al., 2006), the neurodegenerative process of the PCs is dramatically rapid and severe and almost all of them disappear 1 month after birth. In addition to *pcd*, a monogenic biallelic variant in the gene encoding CCP1was very

Abbreviations: CCP1, Cytosolic carboxypeptidase 1; DFC, Dense fibrillar component; FC, Fibrillar centers; NCL, Nucleolin; NLS, Nuclear location signal; PC, Purkinje cell; Pcd, Purkinje cell degeneration; SG, Stress granules

* Corresponding author at: Department of Anatomy and Cell Biology, Faculty of Medicine, Avd. Cardenal Herrera Oria s/n, 39011 Santander, Spain.
E-mail address: lafargam@unican.es (M. Lafarga).

[1] Both authors equally contributed to this work.

https://doi.org/10.1016/j.nbd.2019.03.017
Received 19 December 2018; Received in revised form 25 February 2019; Accepted 20 March 2019
Available online 21 March 2019
0969-9961/

recently identified in a cohort of patients with infantile-onset neurodegeneration and cerebellar atrophy, linking loss of functional CCP1 to human neurodegeneration (Shashi et al., 2018).

Although the loss of function of the *Agtpbp1* gene causes a severe nuclear phenotype in affected neuronal populations (Baltanás et al., 2011a,b; Shashi et al., 2018; Valero et al., 2006), the potential nuclear functions of CCP1 are unknown. Our previous studies demonstrated that during this pre-degenerative stage, PCs show a progressive large-scale reorganization of chromatin, accumulation of DNA damage, and disruption of nucleoli and Cajal bodies in addition to cytoplasmic alterations in protein synthesis machinery (Baltanás et al., 2011a, 2011b).

The nucleolus is a membraneless organelle with physicochemical and structural features that facilitate molecular interactions to catalyze several essential functions for cellular homeostasis (Boisvert et al., 2007; Tiku and Antebi, 2018). The nucleolus is composed of three major structural and functional components: i) fibrillar centers (FC, concentrate RNA pol I transcription machinery), ii) dense fibrillar component (DFC) that closely surrounds FC as FC-DFC units (pre-rRNA synthesis and processing), and iii) granular component (GC, pre-ribosome assembly) (Parlato and Kreiner, 2013; Raška et al., 2006; Tiku and Antebi, 2018). Although the best-known function of the nucleolus is the synthesis and maturation of ribosomal RNAs (rRNAS) and their assembly into pre-ribosomal particles (Parlato and Kreiner, 2013; Raška et al., 2006; Tiku and Antebi, 2018), proteomic analysis reveals that only around 30% of nucleolar proteins are implicated in ribosome biogenesis (Ahmad et al., 2009). Indeed, the nucleolus is a central hub in both coordinating cellular stress responses, including the p53-mediated signaling, and the maintenance of genome architecture and stability, as well as the cell cycle control and immobilization of nuclear proteins (Boulon et al., 2010; Deisenroth et al., 2016). The phosphatase and tension homolog (PTEN), which is a negative regulator of the PI3K/Akt signaling pathway, is also an important sensor of nucleolar stress, and regulates a broad repertoire of cellular functions, including ribosomal biogenesis, chromosome stability and regulation of the DNA damage response (Shen et al., 2007; Song et al., 2012; Zhang et al., 2005).

Nucleolar dysfunction with impairment of RNA Pol I activity, a condition frequently referred as “nucleolar stress” (Boulon et al., 2010; Drygin et al., 2010; Kalita et al., 2008), is associated with several neurodegenerative disorders, including Alzheimer's and Parkinson's diseases, ALS and spinal muscular atrophy (Garcia-Esparcia et al., 2017; Haeusler et al., 2014; Hernández-Ortega et al., 2016; Hetman and Pietrzak, 2012; Parlato and Kreiner, 2013; Rieker et al., 2011; Tapia et al., 2017). For instance, nucleolar stress induced by perturbation of rRNA synthesis after knocking out *Tif1a*, a RNA Pol I coactivator, leads to neurodegeneration in mice (Kreiner et al., 2013; Parlato et al., 2008). Moreover, reduction of rRNA synthesis and nucleolar size occurs during aging, which represents a major risk factor for neurodegenerative disorders (Mattson and Magnus, 2006).

Among major nucleolar proteins involved in ribosome biogenesis, the multifunctional protein NLC, a molecular chaperone highly conserved in all eukaryotic organisms, is predominantly localized to the FC/DFC boundary and DFC (Ginisty et al., 1998). NCL interacts directly with rDNA and pre-rRNA and plays an important role in promoting both pre-rRNA transcription and processing as well as the assembly of pre-ribosomal particles (Cong et al., 2012; Ginisty et al., 1998). Thus, whereas NCL is associated with active ribosomal genes and assists RNA Pol I transcription, the interaction of NCL with pre-rRNA might be necessary for the proper RNA folding and processing (Ogawa and Baserga, 2017). Other important roles of NCL are the regulation of mRNA and the DNA damage response. Thus, NCL has effect on both turnover and translation of its target mRNAs, including several stress-responsive transcripts (Abdelmohsen and Gorospe, 2012; Yang et al., 2002), and also interacts with proteins involved in DNA repair process of double strand breaks (DSBs, for review (Ogawa and Baserga, 2017). Under certain cellular stress conditions, NCL may be redistributed from the nucleus to the nucleoplasm in a p53-dependent manner (Daniely et al., 2002).

Interestingly, mislocalization of NCL is associated with different neurodegenerative diseases. In ALS and frontotemporal dementia, NCL binds specifically to the hexanucleotide repeat expansion (GGGGCC) G-quadruplex of the *C9orf72* gene. The binding of G-quadruplex of abortive *C9orf72* transcripts to NCL associates with loss of nucleolar integrity and mislocalization of NCL away from the nucleolus to the nucleoplasm, resulting in a nucleolar stress and nucleolar pathology (Haeusler et al., 2014; O'Rourke et al., 2015). Similarly, in polyglutamine (PolyQ) neurodegenerative disorders, such as Huntington's disease and several spinocerebellar ataxias, the interaction between the expanded *CAG* RNA and the NCL prevents pre-RNA transcription and induces nucleolar stress (Tsoi et al., 2012; Zhang et al., 2018). Moreover, NCL interacts with the fragile X mental retardation protein forming a protein complex that appears to be involved in the nucleocytoplasm shuttling of NCL (Taha et al., 2014). Finally, α-synuclein and DJ-1, two critical proteins in Parkinson's disease pathogenesis, also interact with NCL (Jin et al., 2007). Collectively, these studies support an important role of NCL protein in the neuronal dysfunction associated with several neurodegenerative disorders.

The results reported here demonstrate the nucleolar reorganization of NCL and its partial translocation to chromatin and cytoplasm in degenerating PCs from the *pcd* mutant mouse. This NCL shift is associated to p53-dependent nucleolar stress, and results in reduced rate of pre-rRNA processing, chromosome instability and accumulation of poly (A) RNAs in stress granules (SG). Importantly, nucleolar stress is accompanied by reduced expression of PTEN, that regulates ribosomal biogenesis, chromosome stability and the DNA damage response (Shen et al., 2007; Song et al., 2012; Zhang et al., 2005), three cellular mechanisms mainly affected by the *Agtpbp1* gene mutation in PCs of *pcd* mouse.

2. Materials and methods

2.1. Mouse genotyping

Both WT and *pcd* mice (holding pcd^{1j} mutation) from the C57/DBA strain were purchased from the Jackson Laboratory (Maine, USA). For mouse genotyping, DNA from the tails of the mice was extracted and PCR was performed as previously described (Baltanás et al., 2011a). The animals were kept, handled and sacrificed in the NUCLEUS animal facility of the University of Salamanca according with current European and Spanish legislations, and the Bioethical Committee of the University of Salamanca approved the experiments.

2.2. Tissue fixation and fluorescence labeling

Mice of both genotypes were deeply anesthetized and perfused with heparinized saline for 1 min and fixative solution containing 4% paraformaldehyde and 0.2% saturated picric acid in 0.1 M phosphate buffer (PB), pH 7.4, for 15 min. After perfusion, the vermis of the cerebellum was dissected out and post-fixed in the same solution for 2 h at room temperature (RT). The tissue blocks were washed in PB and cryoprotected with 30% sucrose overnight at 4 °C until they sank. 30-μm-thick sagittal sections were cut using a freezing-sliding microtome (Leica Frigomobil, Jung SM 2000, Nussloch, Germany) and the slices were collected in PB.

Sections were rinsed in phosphate-buffered saline (PBS; 3 × 5 min), and incubated with propidium iodide (PI, 1:1000) for 1 h at RT. Finally, the sections were washed in PBS, mounted, and coverslipped with antifade solution. The resulting material was examined with a confocal microscope (Zeiss LSM 510).

2.3. Squash preparations and immunofluorescence

Squash preparations of PCs from fragments of the vermis were obtained as described (Baltanás et al., 2015). Both P20 WT and P20 *pcd* mice (n = 3/genotype) were perfused with 3.7% paraformaldehyde in PBS. The vermis was removed and post-fixed in the same solution for 20 min at RT. Small tissue blocks containing the PCs were isolated and transferred to a drop of PBS on a siliconized slide. A coverslip was then applied to the top of the slide, and the tissue was squashed by mechanical pressure with a histological needle to dissociate neuronal perikarya. The preparation was then frozen in dry ice, and the coverslip was removed using a razor blade. With this procedure, most PCs remained adhered to the slide. Cell samples were then sequentially processed in 96% ethanol at 4 °C for 10 min and PBS at 4 °C.

For immunocytochemical studies, the samples were sequentially treated with 0.1 M glycine in PBS for 15 min and 0.5% Triton X-100 in PBS for 45 min at RT. Then, they were incubated with the corresponding primary antibodies overnight at 4 °C, washed with 0.05% Tween 20 in PBS, and incubated for 45 min in the specific secondary antibodies conjugated with FITC or Texas Red (Jackson ImmunoResearch, West Grove, PA), rinsed in PBS, and counterstained with PI or DAPI (1:2000) for 15 min. Finally, the samples were mounted with antifade medium. They were examined with a laser confocal microscope Zeiss LSM 510.

The following primary antibodies were used: rabbit polyclonal antibody anti-53BP1 (1:200, Novus Biologicals), mouse monoclonal antibody anti-γH2AX (1:300, Upstate), rabbit polyclonal anti-H4K20me3 (1:200, Upstate), mouse monoclonal anti-SMN (1:50, BD transduction laboratories), rabbit polyclonal anti-NCL (1:500, Abcam) and mouse monoclonal anti-UBF (1:100, Santa Cruz).

2.4. In situ hybridization

Squash PCs samples from both P20 WT and *pcd* mice were processed for fluorescence *in situ* hybridization (FISH). Preparations were permeabilized with TBS-*E*-SDS for 15 min at 37 °C, washed three times in 6× SSPE-0.1% Tween-20 for 15 min, and incubated with the probe containing tRNA for 3 h at 42 °C in a humidified chamber. An oligo dT (50)-mer, 5′-end labeled with biotin (MWG-Biotech, Germany) was used as a probe for FISH to poly(A) RNA. The hybridization mixture contained 80 ng of oligo dT(50), 2× SSC, 1 mg/ml tRNA, 10% dextran sulfate and 25% formamide. After hybridization, the samples were washed in 6× SSC for 15 min, and then washed in 4× SSC-0.1% Tween 20 for 15 min at RT. The hybridization signal was detected with FITC-avidin for 30 min. For amplification of the hybridization signal, PCs samples were incubated with avidin-biotin for 30 min, washed in 4× SSC-0.1% Tween-20 for 15 min and then incubated with FITC-avidin for 30 min. All samples were mounted with antifade medium.

2.5. Electron microscopy

P20 WT and P20 *pcd* mice (n = 3/genotype) were used to analyze the conventional ultrastructure of PCs. Mice were perfused with 3% glutaraldehyde in 0.1 M PB, pH 7.4. The cerebellum was removed, and the vermis was isolated. 500-μm-thick sagittal sections were obtained using a vibratome (Leica). Then the sections were rinsed in 0.1 M PB, post-fixed in 2% osmium tetroxide diluted in double-strength buffer (containing 3.5% dextrose in 0.2 M PB, pH 7.4), dehydrated in acetone, and embedded in Araldite (Durcupan, Fluka, Switzerland). Ultrathin sections stained with uranyl acetate and lead citrate were examined with a JEOL 201 electron microscope.

For immunoelectron microscopy, the animals were perfused with 3.7% paraformaldehyde in 0.1 M cacodylate buffer for 10 min at RT. Small tissue fragments of the vermis were washed in 0.1 M cacodylate buffer, dehydrated in increasing concentrations of methanol at −20 °C, embedded in Lowicryl K4M at −20 °C, and polymerized with ultraviolet irradiation. Ultrathin sections were mounted on nickel grids and sequentially incubated with 0.1 M glycine in PBS for 15 min, 5% BSA in PBS for 30 min, and the primary mouse monoclonal anti-NCL antibody (1:50, Abcam) for 2 h at 37 °C. After washing, the sections were incubated with the goat anti-mouse IgG secondary antibody coupled to 10-nm gold particles (BioCell, UK, 1:50 in PBS containing 1% BSA) for 1 h at RT. Following immunogold labeling, the grids were stained with lead citrate and uranyl acetate and examined with a JEOL 201 electron microscope. As controls, ultrathin sections were treated as described above in the absence of the primary antibodies.

2.6. Western blot

P15 and P20 WT and *pcd* mice (n = 3/genotype/age) were euthanized and the vermis of the cerebellum was collected and quickly frozen before tissue homogenization in RIPA buffer using GentleMacs® dissociator. 50 μg total protein was loaded in electrophoresis gels and immunoblotting was performed. Primary antibodies used were: rabbit polyclonal anti-CCP1 (1:1000, Proteintech), rabbit polyclonal anti-NCL (1:1000, Abcam), rabbit polyclonal anti-PTEN (1:1000, Abcam), mouse monoclonal anti-p53 (1:500, Cell Signaling) and mouse monoclonal anti-tubulin (1:5000, Sigma).

Values of protein expression were determined using ImageJ software (NIH, USA).

2.7. Real time quantitative PCR

P20 WT and *pcd* mice (n = 3/genotype) were euthanized and the vermis was quickly removed and frozen. RNA was isolated with Trizol and purified with the RNeasy kit (Qiagen, Germany). One μg of RNA was reverse-transcribed to first-strand cDNA using a High Capacity cDNA Reverse Transcription Kit (Life Technologies) using random hexamers as primers. cDNA concentration was measured in a spectrophotometer (Nanodrop Technologies ND-1000) and adjusted to 0.5 μg/μl. For qRT-PCR analyses we used the following gene-specific SYBRGreen-based primers: i) for the expression of rRNAs candidates 45S 5′-gaacggtggtgtgtcgtt-3′ and 5′-gcgtctcgtctcgtctcact-3, for rRNAs containing the mature sequence of 18S 5′-gatggtagtcgccgtgcc-3′ and 5′-ccaaggaaggcagcaggc-3′, and for rRNA precursors containing the 5′-junction span of mature 18S 5′-cgcgcttccttacctggttg-3′ and 5′-ggagaggagcgagcgacc-3′; ii) for the expression of mRNAs of the nucleolar components nucleolin (*Ncl*) 5′-attggggagggaagggaagt-3′and 5′-tcagcacttcgagttgaagca-3′, for UBF (*Ubtf*) 5′-ccgcgcagcatacaaagaat-3′ and 5′-gtggtccggctagacttgg-3′, and for fibrillarin (*Fbl*) 5′-tctggtccctggagagtctg-3′ and 5′-gggttccaggctctgtactc-3′; and iii) for the expression of *Pten* mRNA 5′-ttgttagcctcttgatgtgtgc-3 and 5′-tggtagccaaacggaacttca-3′. Unless otherwise indicated, the results obtained were normalized to mRNA expression of the housekeeping gene *Actinb* that was determined by qRT-PCR using the primers 5′-cagccttccttcttgggtatg-3′and 5′-ggcatagaggtctttacggatg-3. All the analyses were carried out using GraphPad Prim 7 software for Mac. Statistical significance was set at $p < .05$.

3. Results

Several studies have reported that PC death in the *pcd* mice occurs within a time frame from P15 to P45 (Baltanás et al., 2011a,b). By means of cytochemical staining with PI of sagittal cryosections of the vermis we demonstrated a moderate loss of PC bodies at P20 in *pcd* mice in comparison with WT control ones (Supplementary Fig. 1A, B) (8). Since we observed at this period that numerous healthy PCs coexist with different stages of PC degeneration in the cerebellar vermis, we decided to study the variations of the expression pattern of NCL associated with the nucleolar stress response in PCs of *pcd* mice at P20. First, we confirmed the absence of CCP1 protein expression in cerebellar vermis lysates from the *pcd* mice (Supplementary Fig. 1C). By immunofluorescence, we then assessed the γH2AX and 53BP1

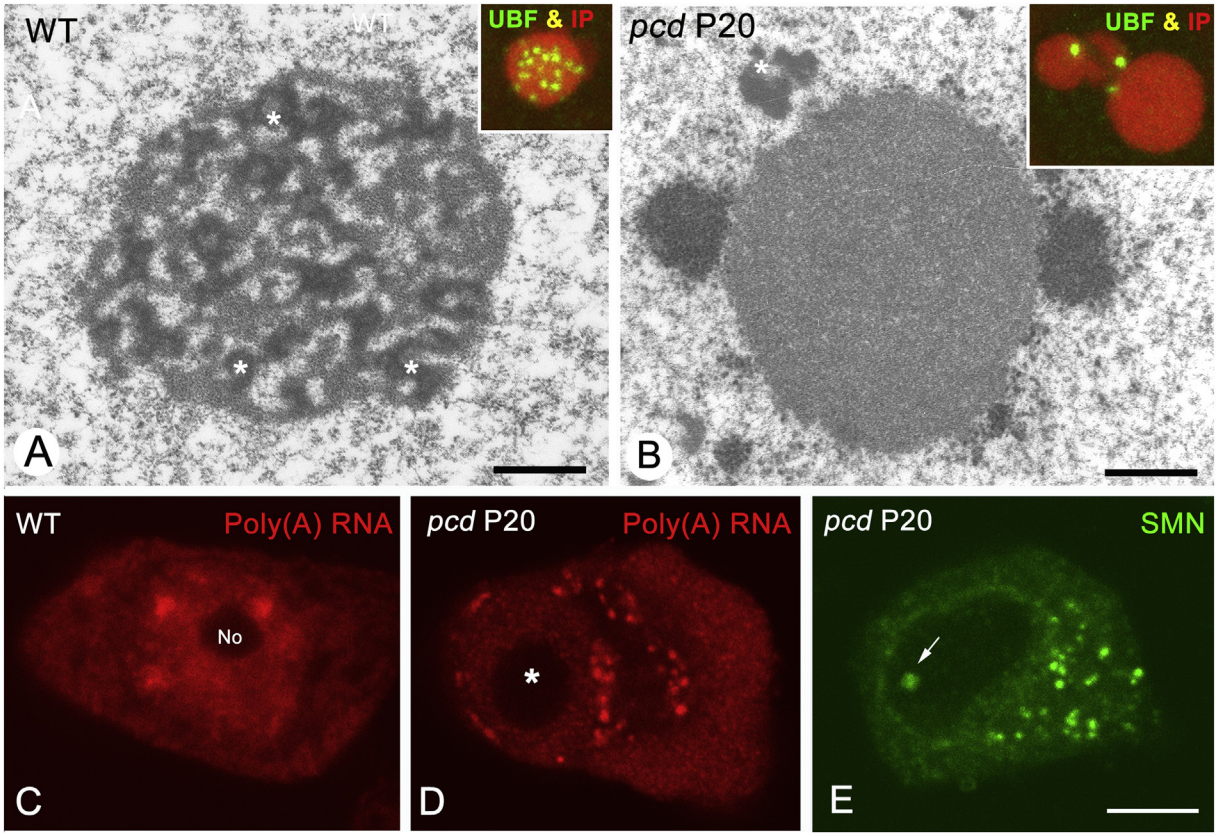

Fig. 1. (A) Representative electron micrographs showing a typical reticulated nucleolus of a PC from a WT mouse with numerous FC/DFC units (asterisks). Inset. Confocal microscopy image of a WT PC immunolabeled for UBF (green) and counterstained with PI. Note the nucleolus with numerous UBF-positive FCs. (B) Electron microscopy image of a mutant PC. Nucleolar fragments of dense fibrillar components appeared attached to a large heterochromatin mass. Inset. Prominent heterochromatin masses counterstained with PI exhibit isolated UBF-positive spots, which are segregated remnants of FC/DFC units, at their surface. Scale bars (A–B): 1 µm. (C–D) *In situ* hybridization for poly(A) RNA in PCs from WT (C) and *pcd* (D) mice. Note in panel C the typical nuclear distribution of polyadenylated mRNAs diffuse in the nucleoplasm, concentrated in nuclear speckles and absent in the nucleolus (No). The cytoplasmic poly(A) RNA signal corresponds to the distribution of protein synthesis machinery. In a degenerating PC (E) nuclear speckles disappear and polyadenylated mRNAs appear concentrated in numerous stress granules, which are also immunostained for the SMN protein (E). Arrow in E indicates a SMN-positive nuclear body identified as a Cajal body. Scale bar: 5 µm. (For interpretation of the references to colour in this figure legend, the reader is referred to the web version of this article.)

immunostaining as indicator of DNA damage. As we previously reported, numerous γH2AX- and 53BP-positive chromatin domains, which tend to coalesce into one large chromatin area, were found in degenerating PCs of the *pcd* mice (Supplementary Fig. 1D–F) (Baltanás et al., 2011a). Moreover, by both electron microscopy and H4K20me3 immunostaining, to detect repressive heterochromatin, we also confirmed the presence of numerous heterochromatin domains distributed throughout the nucleus, which tended to coalesce into a few big heterochromatic regions in PCs of *pcd* mice (Supplementary Fig. 1H).

3.1. *Agtpbp1 gene mutation induces nucleolar fragmentation and perturbation of protein synthesis machinery*

We then addressed the nucleolar integrity by electron microscopy analysis and immunolabeling for the upstream binding factor (UBF), a transcription factor of ribosomal genes that accumulates in FC (Boisvert et al., 2007). While the prominent nucleolus of WT PCs contained numerous FC/DFC units (Fig. 1A, inset), degenerating PCs from *pcd* mice showed a peculiar mechanism of loss of nucleolar integrity including the fragmentation of the nucleolus and the presence of remaining nucleolar fragments spatially linked to big heterochromatin masses (Fig. 1B, inset). This nucleolar behavior was accompanied by the loss of UBF-positive FCs and the segregation of UBF remnants at the periphery of heterochromatin masses (Fig. 1B, inset).

We have previously reported that nucleolar disruption was coupled with perturbation of protein synthesis machinery (Baltanás et al., 2011b). To further analyze this effect, we studied the localization of poly(A) RNAs by *in situ* hybridization. In WT PCs poly(A) RNAs showed a diffuse nuclear distribution, excluding the nucleolus, with higher concentration in nuclear speckles (Fig. 1C), nuclear domains for storage and assembly of splicing factors (Lamond and Spector, 2003). Importantly, a shift of poly(A) RNA distribution pattern was detected in degenerating PCs of *pcd* mice. The changes included loss of nuclear accumulations of poly(A) RNA in nuclear speckles and its cytoplasmic concentration in SGs and, more diffusely, at the marginal cytoplasm (Fig. 1D). SGs also concentrated another of their typical molecular constituents in neurons, the survival motor neuron (SMN) protein (Fig. 1E), which is a facilitator of stress granule formation (Hua and Zhou, 2004). The *de novo* formation of SGs, which accumulates untranslated polyadenylated mRNAs, is consistent with reduced global translation in degenerating PCs of *pcd* mice.

3.2. *Agtpbp1 gene mutation induces the subcellular redistribution of NCL in PCs of pcd mice*

To gain further insight into the nucleolar response in degenerating PCs we analyzed by immunostaining the nucleolar and extranucleolar reorganization of NCL induced by the *Agtpbp1* gene mutation. In WT PCs, NCL concentrated in the prominent round-shaped nucleoli, and was almost undetectable in the nucleoplasm (Fig. 2A–C). Loss of nucleolar integrity in degenerating PCs was reflected by the lobulation and fragmentation of NCL-immunolabeled nucleoli (Fig. 2D–F).

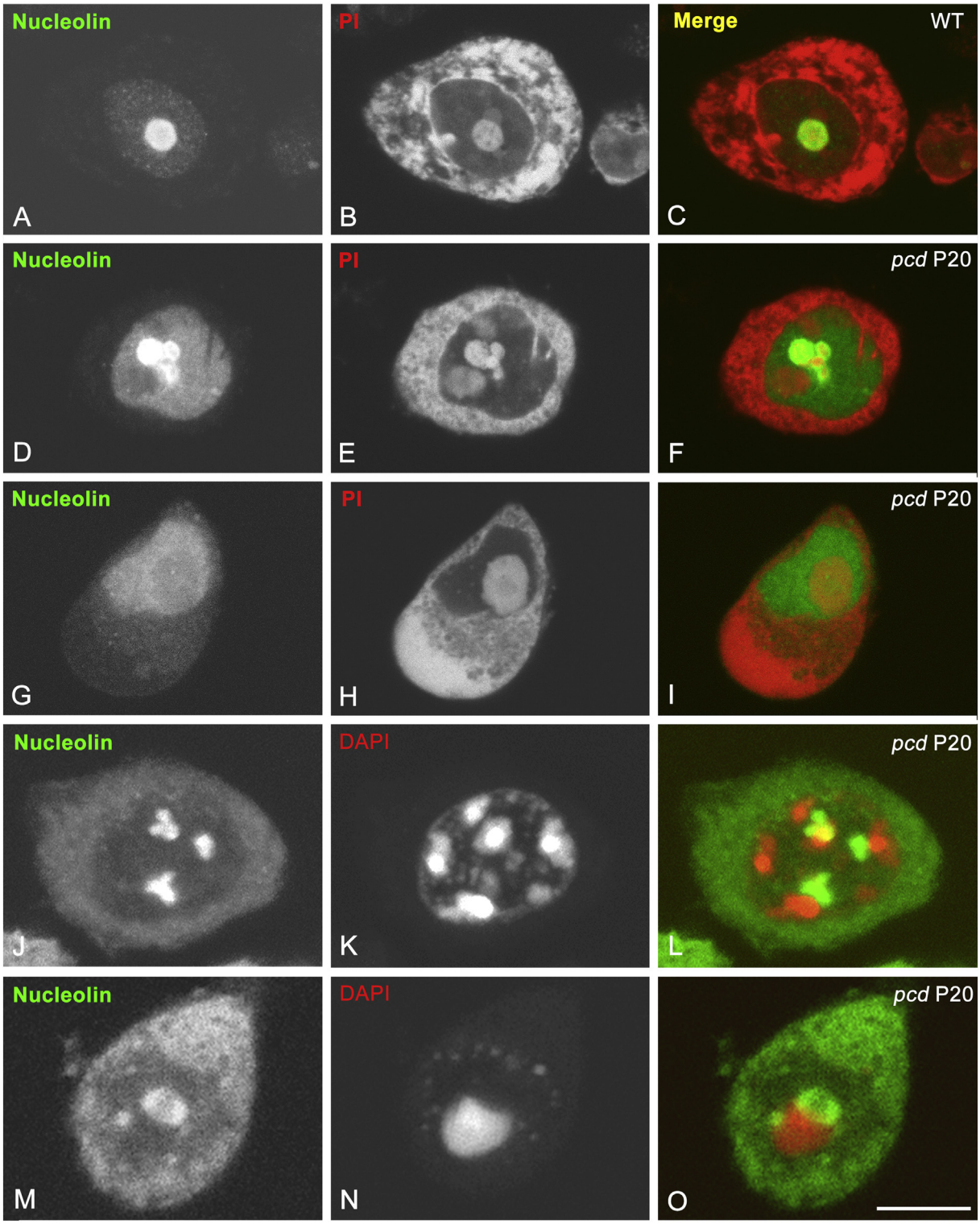

Fig. 2. (A–O) NCL immunolabeling of PCs from P20 WT (A–C) and *pcd* (D–O) mice counterstained with PI (A–I) or DAPI (J–O). The WT PC exhibits a prominent NCL-positive nucleolus and well developed rRNA-rich Nissl substance stained with PI (A–C). Degenerating PCs show lobulation and fragmentation of nucleoli, nucleoplasmic and cytoplasmic accumulation of NCL (D–O). Note the close association of NCL-positive nucleolar fragments with prominent heterochromatin clumps counterstained with DAPI. Scale bar: 10 µm.

Interestingly, a remarkable nucleoplasmic accumulation of NCL was observed in all PCs exhibiting nucleolar alterations and large heterochromatin masses (Fig. 2D–I). Moreover, particularly in neurons exhibiting central chromatolysis, NCL was translocated to the cytoplasm as PC degeneration proceeded (Fig. 2G–L). These changes in NCL staining pattern were associated with the formation of large heterochromatin masses counterstained with PI (Fig. 2D–I), reflecting gene silencing in extensive genome domains. The close spatial association of nucleolar fragments with heterochromatin domains was confirmed in PCs immunolabeled for NCL and counterstained with DAPI (Fig. 2J–O).

Immunoelectron microscopy analysis of NCL in PCs from WT and

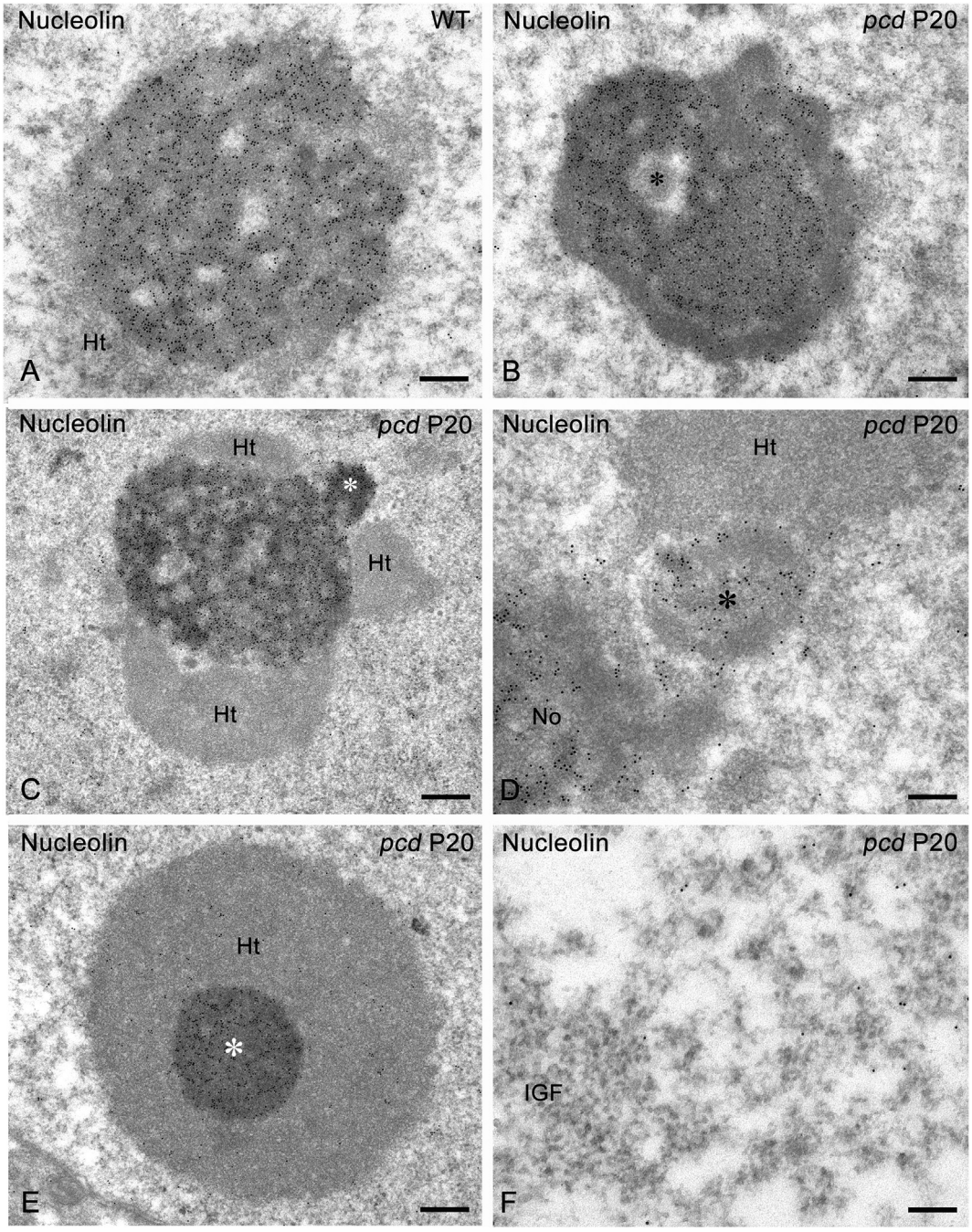

Fig. 3. (A–F) Immunogold electron microscopy for NCL in PCs from P20 WT (A) and *pcd* mice (B—F). (A) Typical reticulated nucleoli of a WT PC showing the preferential distribution of NCL-associated gold particles on the DFC. Ht: nucleolus associated heterochromatin. Scale bar: 0.3 µm. (B) Nucleolar compaction of NCL-positive DFC in the central region of the nucleolus. Note an intranucleolar vacuole containing an INoB (asterisk). Scale bar: 0.3 µm. (C) A nucleolar fragment immunoreactive for NCL (asterisk) appears attached to the nucleolus. Note the presence of three prominent masses of nucleolus-associated heterochromatin (Ht). (D) A nucleolar fragment immunolabeled for NCL (asterisk) appears attached to a mass of heterochromatin (Ht) in the vicinity of the nucleolus (No). Scale bar: 0.3 µm. (E) An intensely NCL-immunolabeled nucleolar remnant (asterisk) appear completely surrounded by heterochromatin (Ht). Scale bar: 0.4 µm. (F) Distribution of NCL in euchromatin domains. Note the absence of gold articles an interchromatin granule cluster (IGC). Scale bar: 150 nm. (For interpretation of the references to colour in this figure legend, the reader is referred to the web version of this article.)

pcd mutant mice confirmed the subnuclear redistribution of NCL observed with the immunofluorescence analysis. Thus, WT PCs exhibited a typical reticulated nucleolar pattern of NCL corresponding to the organization of the DFC around of FCs (Fig. 3A). Several changes in NCL localization were detected in degenerating PCs. They included nucleolar compaction of the DFC with loss of FCs, formation of small cavities, which contained an electron-dense NCL-negative intranucleolar body (INoB, (Tapia et al., 2017) and the appearance of NCL-positive nucleolar fragments frequently associated with the heterochromatin masses (Fig. 3B–D). The formation of large heterochromatin masses, some of them attached to the nucleolar surface or even completely surrounding an NCL-immunoreactive nucleolar fragment, was a prominent finding in degenerating PCs (Fig. 3C–E). Interestingly, immunoelectron microscopy demonstrated de specific extranucleolar redistribution of NCL in the structured chromatin (Fig. 3F). Indeed, NCL was excluded from the interchromatin granule clusters,

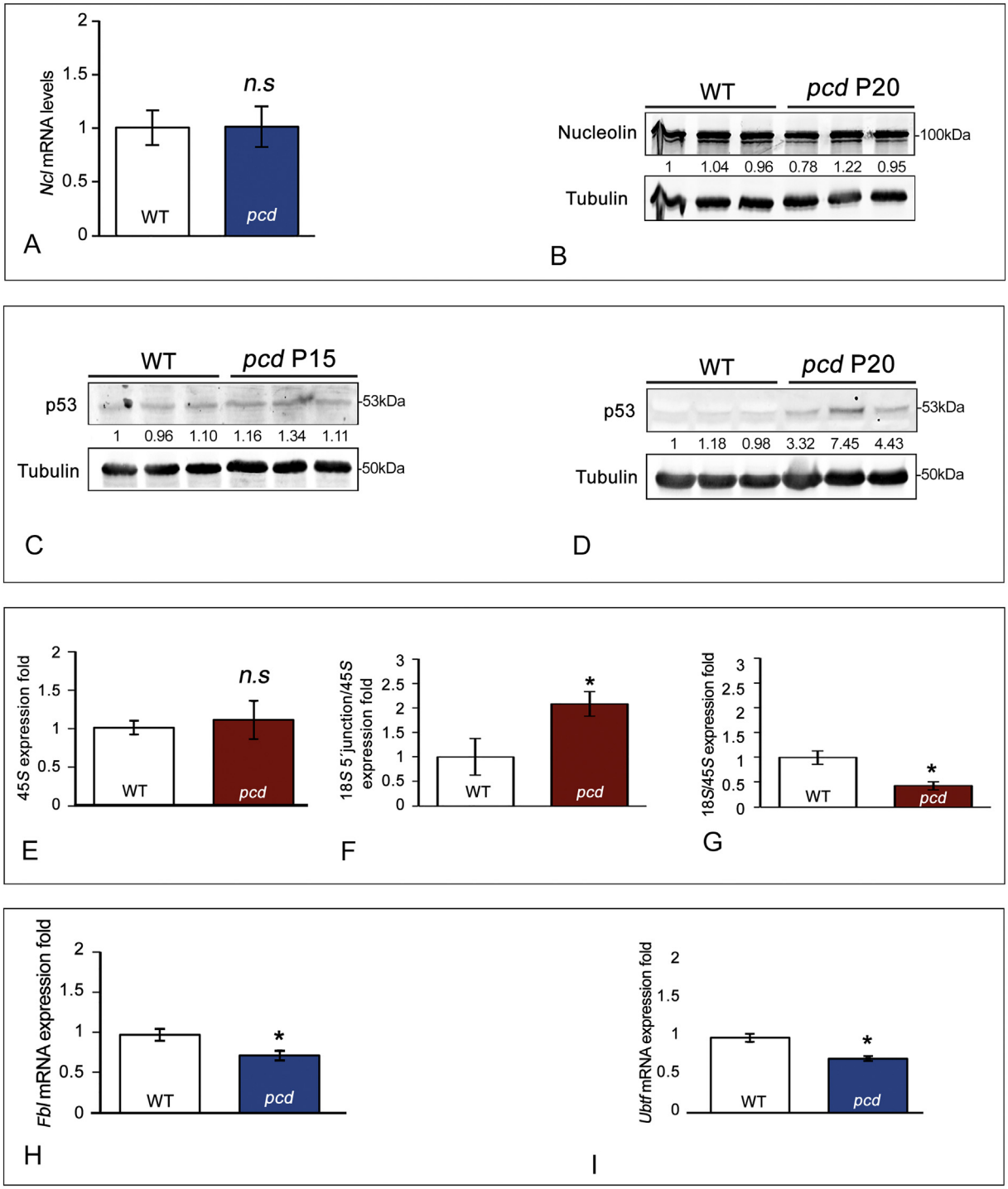

Fig. 4. (A) RT-qPCR of the relative levels of *Ncl* mRNA expression in RNA extracts of the cerebellar vermis from P20 WT and *pcd* mice. No significant differences (n.s) were found when comparing WT and *pcd* samples. (B) Western blot analyses of NCL protein levels in cerebellar vermis lysates from WT and *pcd* mice at P20 (C). No significant differences were found between both experimental groups at any stage. (C-D) Western blots of p53 protein levels in cerebellar vermis lysates from WT and *pcd* mice at P15 (C) and P20 (D). Whereas no significant differences were found between WT and *pcd* samples at P15, p53 expression significantly increased in *pcd* samples at P20. Protein levels were normalized to tubulin and the fold increase estimated. (E–G) RT-qPCR of the relative levels of the pre-rRNA precursor 45S, mature 18S rRNA and a 18S-5' ETS junction intermediate in RNA extracts of cerebellar vermis from P20 WT and *pcd* mice. No significant differences of pre-rRNA 45S were found between WT and *pcd* samples (E). In contrast, the expression of the mature 18S rRNA significantly decrease (G) in parallel with an increase of the 18S-5' ETS junction intermediate (F). $*p < .05$ (C). The bars represent the mean ± SD. RT-qPCR analyses were always confirmed in triplicate. (H—I) RT-qPCR determination of the relative levels of *Fbl* (H) and *Ubtf* (I) mRNAs in the cerebellar vermis from WT and *pcd* mice at P20. Both mRNA levels were significantly reduced in *pcd* samples. $*p < .05$. The bars represent the mean ± SD. RT-qPCR analyses were always confirmed in triplicate.

chromatin free nuclear compartments corresponding to nuclear speckles of splicing factors at light microscopy level (Lamond and Spector, 2003).

We then investigated whether the redistribution of NCL in PCs from *pcd* mice correlated with variations in mRNA and protein levels of NCL. By P20, no-significant differences were found in neither in *Ncl* mRNA expression nor NCL protein levels in the cerebellar vermis between WT and *pcd* experimental groups (Fig. 4A, B). These finding indicates that the subcellular redistribution of NCL, rather than a variation of its mRNA and protein expression, is involved in the dysfunction of PCs of the *pcd* mice. Nonetheless, it should be noted that these mRNA and protein data are referred to the whole cerebellar vermis, not only to PCs. Consequently, the possible contribution of other cerebellar neuronal or glial populations cannot be excluded.

Next, we investigated whether the nucleolar stress response was dependent on p53 (Deisenroth and Zhang, 2010). Interestingly, p53 protein levels were increased significantly in the *pcd* cerebella at P20 (Fig. 4D). In order to analyze whether the changes of p53 were a direct consequence of *Agtpbp1* mutation we analyzed its expression at p15, prior to PC degeneration. At this period no variations in protein expression were detected (Fig. 4C), supporting a p53-dependent nucleolar stress response directly associated with the neurodegenerative process of PCs, rather than with *Agtpbp1* mutation itself.

3.3. *Agtpbp1* gene mutation affects pre-rRNA processing in the cerebellum

To further investigate the impact of *Agtpbp1* gene mutation on the nucleolar functions, particularly on pre-rRNA synthesis and processing, we used RT-qPCR to analyze changes in mRNA expression levels of the pre-rRNA 45S, mature rRNA 18S and an intermediate precursor of the 18S rRNA, the 18S-5' ETS (external transcribed sequence) junction rRNA, which corresponds to a sequence junction between the ETS and contiguous mature 18S rRNA. Interestingly, whereas non-significant changes were detected in the expression of pre-rRNA 45S, the relative abundance of the intermediate 18S-5' ETS junction rRNA and mature 18S rRNA, with respect to 45S precursor, significantly increased and decreased, respectively, in P20 *pcd* cerebellar extracts as compared with WT counterparts (Fig. 4E–G). These data support a dysfunction of pre-rRNA processing resulting in the accumulation of an intermediate precursor of the 18S rRNA and the consequent reduction in its mature form. Consistent with this view, we found a significant decrease of the mRNA encoding fibrillarin (Fig. 4H), a key nucleolar protein of the DFC specifically involved in pre-rRNA processing (Boisvert et al., 2007; Raška et al., 2006). Moreover, the expression of *UBTF* mRNA, which encodes the transcription factor UBF (Boisvert et al., 2007), showed a moderate, but significant, reduction in *pcd* cerebella as compared with WT samples (Fig. 4I).

3.4. PTEN expression is affected during PC degeneration process

Recently, the canonical functions of PTEN as a negative regulator of the PI3K/Akt signaling pathway, have been expanded to include phosphatase-independent activities with special relevance in nuclear functions such as chromosome stability and DNA repair (Shen et al., 2007). PTEN is preferentially expressed in PCs and olfactory mitral neurons (Lachyankar et al., 2000), two cellular targets of *Agtpbp1* gene mutation. Moreover, the alternatively translated isoform PTENβ interacts with NCL and regulates ribosomal gene transcription (Liang et al., 2017). Taken together, these data prompted us to investigate whether the reorganization of NCL associated with changes in PTEN expression. By P20, RT-qPCR measurement of the relative abundance of *Pten* mRNA showed a significant reduction in *pcd* cerebellar vermis extracts as compared with WT samples (Fig. 5A). Similarly, protein levels of PTEN decreased significantly in cerebellar lysates from *pcd* mice in comparison with WT cerebella at P20, but non-significant differences were observed at P15, prior to PC degeneration stage (Fig. 5B). Importantly, two cellular manifestations of PTEN loss, chromosomal reorganization and accumulation of DNA damage, are typical features of degenerating PCs in *pcd* mice (Baltanás et al., 2011a). Indeed, *in situ* hybridization of telomeric DNA in combination of immunostaining for γH2AX revealed a normal distribution of telomeric spots throughout the nucleus of control WT PCs (Fig. 5C), and the dramatic loss of chromosome stability with clustering and fusion of telomeres in DNA damaged chromatin domains in PCs samples from *pcd* mice (Fig. 5D, E).

4. Discussion

Here we reported that the *Agtpbp1* gene mutation-induced PC degeneration alters the nucleolar localization of NCL, induces p53-dependent nucleolar stress, dramatically changes chromatin architecture, interferes with the translational activity leading to the formation of SGs, and downregulates PTEN expression. Curiously, this severe cellular phenotype is apparently unrelated to the well-established function of the *Agtpbp1* gene product, the carboxypeptidase CCP1, in microtubule stabilization (Gilmore-Hall et al., 2018; Kalinina et al., 2007; Zhou et al., 2018). Nonetheless, although the potential nuclear functions of CCP1 are unknown, the cellular alterations reported here and previously in PCs and mitral cells harboring *Agtpbp1* gene mutation (Baltanás et al., 2011b, 2011a; Valero et al., 2006) suggest that CCP1 is a multifunctional protein with potential regulatory roles in nuclear function and chromosome stability. In this vein, it has been reported the coexpression and interaction of *Agtpbp1* and the amyotrophic lateral sclerosis (ALS)-linked gene *C90rf72* suggesting that *Agtpbp1* serves as a *C90rf72* interacting partner contributing to regulate several important neuronal functions (Kitano et al., 2015).

The *pcd* mutation is a model of ataxic mice that shares clinical and histopathological manifestations of inherited human spinocerebellar ataxias, such as defective motor coordination and degeneration and loss of PCs (Lim et al., 2006; Wang and Morgan, 2007). In fact, it has been very recently described that the loss of CCP1 expression induces infantile-onset neurodegeneration affecting cerebellum, spinal motor neurons and peripheral nerves (Shashi et al., 2018). Bioinformatic analysis of the protein interactome network in inherited cerebellar ataxias with PC degeneration revealed that several ataxia proteins are implicated in nuclear functions (Lim et al., 2006). Accordingly, disruption of the nucleolus with nucleolar stress and loss of chromosomal integrity in PCs are cardinal features of the ataxic *pcd* mice (Baltanás et al., 2011a,b). Given that the pivotal role of the nucleolus in coordinating cellular stress response and ribosome biogenesis, nucleolar stress is emerging as an important physiopathological mechanism shared by a wide-range of neurodegenerative disorders (Garcia-Esparcia et al., 2017; Haeusler et al., 2014; Hernández-Ortega et al., 2016; Hetman and Pietrzak, 2012; Parlato and Kreiner, 2013; Rieker et al., 2011; Tapia et al., 2017).

Our results indicate that the mutation of the *Agtpbp1* gene in PCs induces, either directly or indirectly, a p53-dependent nucleolar stress with nucleolar fragmentation, mislocalization of NCL and perturbation of pre-rRNA processing. As far as we know, the present study provides the first analysis of NCL distribution in WT PCs and its nucleoplasmic and cytoplasmic mislocalization in degenerating PCs. Due to the high affinity for nucleolar components, NCL is localized almost exclusively within the nucleolus where it participates in several steps of ribosome biogenesis (Abdelmohsen and Gorospe, 2012; Ginisty et al., 1999). NCL has a nuclear localization signal (NLS) and shuttles between the nucleus and cytoplasm, although only a very small amount of NCL is detected in the cytoplasm due to its rapid and efficient nuclear re-import (Borer et al., 1989; Schmidt-Zachmann and Nigg, 1993).

In the case of *pcd* mice, our results show that the nucleoplasmic mislocalization of NCL is shared by all PCs exhibiting neurodegenerative signs such as nucleolar fragmentation and massive heterochromatinization. Since both mRNA and protein levels of NCL were preserved in the cerebellar vermis of *pcd* mice, we thought that the

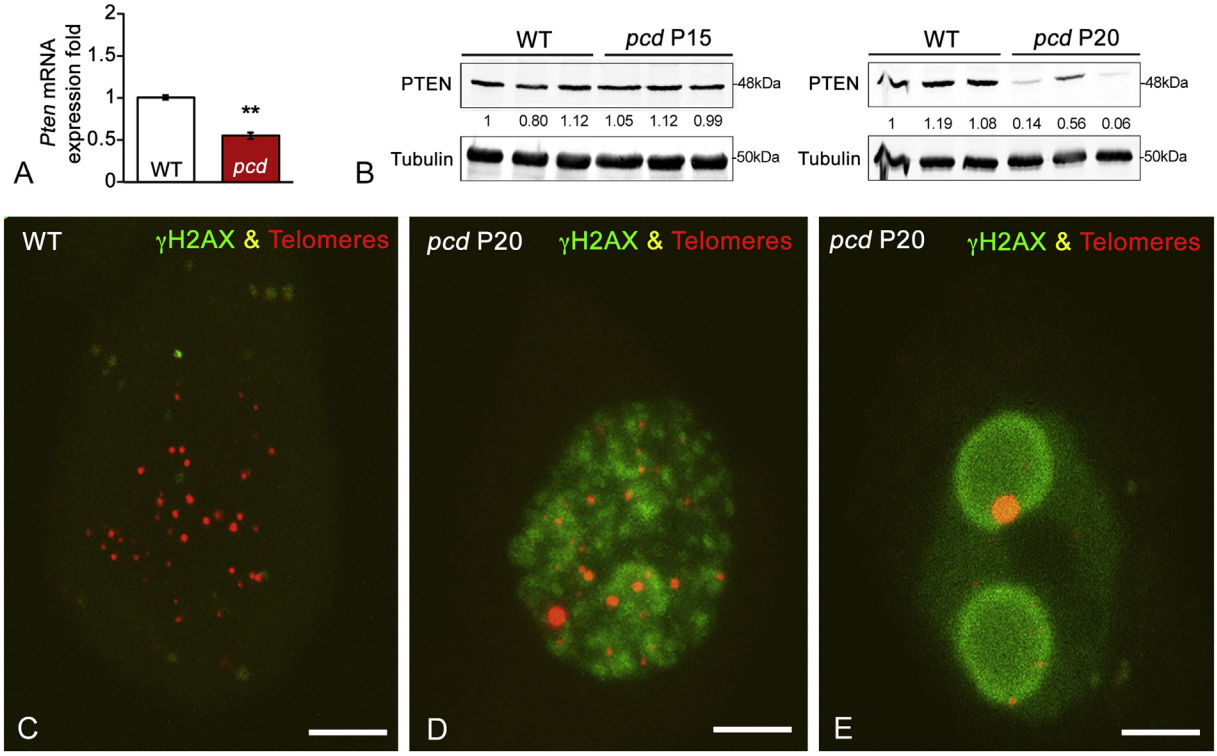

Fig. 5. (A) RT-qPCR of the relative levels of *Pten* mRNA in RNA extracts of cerebellar vermis from WT and *pcd* mice at P20 (n = 3/genotype). A significant decrease was found in *pcd* samples. Data are expressed as mean ± SD. $^{**}p < .01$ (B) Western blots analysis of PTEN protein levels in cerebellar vermis lysates from WT and *pcd* mice at P15 and P20. Whereas no significant differences were found between WT and *pcd* samples at P15, PTEN expression significantly decreased in *pcd* samples at P20, during the degeneration phase of PCs. Protein levels were normalized to tubulin and the fold increase estimated. (C–E) *In situ* hybridization for telomeric DNA in combination with γH2AX immunostaining in PCs from a WT and *pcd* mice at P20. Numerous telomeric spots appear randomly distributed throughout the nucleus in a control PC lacking γH2AX immunostaining (C). (D) As PC degeneration proceeds, the number of telomeric spots decreased and tended to coalesce in larger telomeric spots. (E) At later stages of PC degeneration most telomeres become spatially aggregated into a giant spot. Scale bars: 5 μm.

notable increase of the nucleoplasmic pool of NCL presumably reflects the loss of NCL affinity for nucleolar ligands and might serve as a reliable sensor of nucleolar stress. Consistent with this view, in non-neuronal populations, mobilization of NCL from the nucleolus to the nucleoplasm occurs in a p53-dependent manner in response to certain stress conditions that perturb global transcription, including heat shock, γ-irradiation and treatment with camptothecin and actinomycin D (Daniely et al., 2002; Perlaky et al., 1997). Our finding of a close relationship between nucleolar stress and nucleoplasmic redistribution of NCL is also consistent with the essential role of NCL in two groups of neurodegenerative disorders: polyQ diseases and *C9orf72* gene-linked ALS and frontotemporal dementia. Thus, NCL binds specifically with the expanded *CAG* RNA of polyQ diseases and with the G-quadruplex of abortive *C9orf72* transcripts. Both pathological interactions displace NCL from the nucleolus, resulting in its nucleoplasmic mislocalization and impairment of rRNA transcription with nucleolar stress (Haeusler et al., 2014; O'Rourke et al., 2015; Tsoi et al., 2012). Regarding the cytoplasmic accumulation of NCL, it likely reflects a defective nuclear import of the protein associated with the global perturbation of PC homeostasis. Cytoplasmic accumulation of NCL has also been reported in adenovirus-infected cells and interpreted as a viral mechanism to subvert nucleolar functions (Matthews, 2001). Finally, NCL mislocalization may be involved in the defective DNA repair observed in PCs of the *pcd* mice. In fact, it is well known that the multifunctional NCL has also a role in the DNA damage response induced by DSBs. This NCL function may be governed by p53 and is mediated by its direct interaction with several factors of the DNA damage signaling and repair pathways (Daniely et al., 2002; Kobayashi et al., 2012). Therefore, in addition to the contribution of NCL to nucleolar stress in degenerating PCs, its role in the DNA damage response opens a new research horizon in neurodegenerative disorders with defective DNA repair.

The induction of a nucleolar stress response in PCs of the *pcd* mice is supported by the loss of nucleolar integrity with nucleolar fragmentation (Baltanás et al., 2011b), nucleolar detention of proteins in INoBs and defective rRNA processing. Interestingly, the restructuration of nucleolar architecture with loss of FC/DFC units and the formation of NCL-free INoBs observed in stressed PCs, besides their implication in rRNA synthesis and processing, may also be associated with a nucleolar sequestration of certain proteins, depriving them of their dynamic access and interactions with their corresponding cellular effectors (Lam and Trinkle-Mulcahy, 2015). Thus, in cultured cells, it has been shown that in response to cellular stresses certain proteins carrying a nucleolar detention sequence are immobilized within a “detention center” of the restructured nucleolus (Audas et al., 2012; Lam and Trinkle-Mulcahy, 2015). Moreover, we have previously reported that nucleolar stress induces the retention of SUMO-conjugated proteins in transcription-free INoBs in cultured cells and spinal cord motor neurons from a spinal muscular atrophy murine model (Brun et al., 2017; Tapia et al., 2017).

It is of interest the affectation of rRNA processing detected by RT-qPCR analysis in the cerebellar vermis of *pcd* mice. The reduction of mature 18S rRNA, associated with an increase in its 18S-5’ ETS junction intermediate, suggests a defective processing of the pre-rRNA, particularly of the first step involving a cleavage of the precursor within the 5’ ETS. Importantly, previous studies have demonstrated that NCL catalyzes this 5’ ETS processing by direct interaction with both pre-rRNA and the U3 snoRNP (Ginisty et al., 1999, 2000). Previous studies have shown that the U3 snoRNP binds to nascent pre-rRNA and is required for two early maturation steps of 18S rRNA: cleavage of the precursor and methylation of ribose moieties of ribonucleotides (Dragon et al., 2002; Kiss-László et al., 1996). The dysfunction of pre-

rRNA processing in the *pcd* cerebellar vermis is also supported by the drop in the transcription rate of *Ubtf* and *Fbl* genes encoding UBF and fibrillarin, respectively. Given that fibrillarin is an essential core protein of the U3 snoRNP with methyltransferase activity (Baserga et al., 1991), its reduced mRNA expression in the cerebellar vermis of *pcd* mice might contribute to dysfunction of pre-rRNA processing.

Collectively, the changes associated with the nucleolar stress in degenerating PCs are consistent with defective ribosome biogenesis and translation activity, as revealed by the disassembly of polyribosomes into mRNA-free monoribosomes (Baltanás et al., 2011b) and the formation of poly(A) RNA-rich SGs, two cellular responses that were not observed in WT PCs. In particular, the formation of SGs clearly reflects a cellular stress condition with local sequestration of polyadenylated mRNAs and certain RNA-binding proteins, including SMN, under translational inhibition (Anderson and Kedersha, 2008; Hua and Zhou, 2004). Overactive SG formation has been linked to neurodegeneration in ALS and tautopathies in which there is an abnormal aggregation of pathological proteins such as TDP-43 or tau (Wolozin, 2012).

It is noteworthy that the reduction of both mRNA and protein levels of PTEN in the cerebellar vermis of *pcd* mice is coincident with the period of time when the PC degeneration takes place and with the peak of A*gtpbp1* gene expression occurs in the cerebellar vermis under physiological conditions (Baltanás et al., 2013). In the central nervous system, PTEN is preferentially expressed in neuronal targets of *pcd* mutation, particularly mitral cells and PCs, and it has been implicated in neuronal differentiation, plasticity and injury (Kwak et al., 2010; Lachyankar et al., 2000). Although PTEN plays a key role in cancer acting as tumor-suppressor, it is also emerging as a factor involved in some neurological disorders (Kwak et al., 2010). Of great relevance is the nuclear function of PTEN that appears to be unrelated with its well-described role in the PI3K/AKT signaling pathway. Thus, *Pten*-deficient MEFs show severe chromosome instability and exhibit a great incidence of spontaneous DSBs (Shen et al., 2007). PTEN regulates chromosome integrity *via* its direct interaction with centromeric proteins and also induces the expression of the DNA repair factor RAD51 (Shen et al., 2007). In this context, the alteration of chromosome architecture, with a dramatic rearrangement of telomeres, and the accumulation of DNA damage reported here and previously (Baltanás et al., 2011a), are nuclear hallmarks of PC degeneration in the *pcd* mice. Although future studies are required to elucidate the nuclear mechanisms of chromosome instability in degenerating PCs, our results suggest that PTEN plays an important role in maintaining chromosome architecture.

5. Conclusions

In conclusion, nucleolar stress with fragmentation of the nucleolus and NCL mislocalization, associated with impairment of pre-rRNA processing, are key features of the nucleolar PC-phenotype induced by the *Agtpbp1* gene mutation. This nucleolar stress seems to be a key component in the pathophysiology of cerebellar ataxia in the *pcd* mouse. Nucleolar stress is emerging as an important factor in a growing list of neurodegenerative disorders. The modulation of nucleolar function is an accessible target for drug development, which has already been exploited in cancer therapy (for review, (Hein et al., 2013). Similarly, the nucleolus and ribosome biogenesis will probably soon emerge as an untapped potential neuroprotective target in neurodegenerative disorders.

Supplementary data to this article can be found online at https://doi.org/10.1016/j.nbd.2019.03.017.

Acknowledgements

The authors declare no conflict of interest. The authors wish to thank Raquel García-Ceballos for technical assistance. This work was supported by the following grants: “Instituto de Salud Carlos III” (CIBERNED, CB06/05/0037) and CIBERONC (CB16/12/00352), “Instituto de Investigación Valdecilla” (IDIVAL, Santander, Spain), FIS PI16/02137 from ISCIII and SAF2016-79668-R (MINECO, Spain), SA043U16 (UIC076) and SA030P17 (UIC217) from JCyL (Spain).

References

Abdelmohsen, K., Gorospe, M., 2012. RNA-binding protein nucleolin in disease. RNA Biol. 9, 799–808. https://doi.org/10.4161/rna.19718.

Ahmad, Y., Boisvert, F.-M., Gregor, P., Cobley, A., Lamond, A.I., 2009. NOPdb: nucleolar proteome database—2008 update. Nucleic Acids Res. 37, D181–D184. https://doi.org/10.1093/nar/gkn804.

Anderson, P., Kedersha, N., 2008. Stress granules: the Tao of RNA triage. Trends Biochem. Sci. 33, 141–150. https://doi.org/10.1016/j.tibs.2007.12.003.

Audas, T.E., Jacob, M.D., Lee, S., 2012. Immobilization of proteins in the nucleolus by ribosomal intergenic spacer noncoding RNA. Mol. Cell 45, 147–157. https://doi.org/10.1016/j.molcel.2011.12.012.

Baltanás, F.C., Casafont, I., Lafarga, V., Weruaga, E., Alonso, J.R., Berciano, M.T., Lafarga, M., 2011a. Purkinje cell degeneration in *pcd* mice reveals large scale chromatin reorganization and gene silencing linked to defective DNA repair. J. Biol. Chem. 286, 28287–28302. https://doi.org/10.1074/jbc.M111.246041.

Baltanás, F.C., Casafont, I., Weruaga, E., Alonso, J.R., Berciano, M.T., Lafarga, M., 2011b. Nucleolar disruption and Cajal body disassembly are nuclear hallmarks of DNA damage-induced neurodegeneration in Purkinje cells. Brain Pathol. 21, 374–388. https://doi.org/10.1111/j.1750-3639.2010.00461.x.

Baltanás, F.C., Berciano, M.T., Valero, J., Gómez, C., Díaz, D., Alonso, J.R., Lafarga, M., Weruaga, E., 2013. Differential glial activation during the degeneration of Purkinje cells and mitral cells in the PCD mutant mice. Glia 61, 254–272. https://doi.org/10.1002/glia.22431.

Baltanás, F.C., Valero, J., Alonso, J.R., Berciano, M.T., Lafarga, M., 2015. Nuclear signs of pre-neurodegeneration. In: Clifton, N.J. (Ed.), Methods in Molecular Biology, pp. 43–54. https://doi.org/10.1007/978-1-4939-2152-2_4.

Baserga, S.J., Yang, X.D., Steitz, J.A., 1991. An intact Box C sequence in the U3 snRNA is required for binding of fibrillarin, the protein common to the major family of nucleolar snRNPs. EMBO J. 10, 2645–2651.

Blanks, J.C., Mullen, R.J., Lavail, M.M., 1982. Retinal degeneration in thepcd cerebellar mutant mouse. II. Electron microscopic analysis. J. Comp. Neurol. 212, 231–246. https://doi.org/10.1002/cne.902120303.

Boisvert, F.-M., van Koningsbruggen, S., Navascués, J., Lamond, A.I., 2007. The multifunctional nucleolus. Nat. Rev. Mol. Cell Biol. 8, 574–585. https://doi.org/10.1038/nrm2184.

Borer, R.A., Lehner, C.F., Eppenberger, H.M., Nigg, E.A., 1989. Major nucleolar proteins shuttle between nucleus and cytoplasm. Cell 56, 379–390.

Boulon, S., Westman, B.J., Hutten, S., Boisvert, F.-M., Lamond, A.I., 2010. The nucleolus under stress. Mol. Cell 40, 216–227. https://doi.org/10.1016/j.molcel.2010.09.024.

Brun, S., Abella, N., Berciano, M.T., Tapia, O., Jaumot, M., Freire, R., Lafarga, M., Agell, N., 2017. SUMO regulates p21Cip1 intracellular distribution and with p21Cip1 facilitates multiprotein complex formation in the nucleolus upon DNA damage. PLoS One 12, e0178925. https://doi.org/10.1371/journal.pone.0178925.

Cong, R., Das, S., Ugrinova, I., Kumar, S., Mongelard, F., Wong, J., Bouvet, P., 2012. Interaction of nucleolin with ribosomal RNA genes and its role in RNA polymerase I transcription. Nucleic Acids Res. 40, 9441–9454. https://doi.org/10.1093/nar/gks720.

Daniely, Y., Dimitrova, D.D., Borowiec, J.A., 2002. Stress-dependent nucleolin mobilization mediated by p53-nucleolin complex formation. Mol. Cell. Biol. 22, 6014–6022.

Deisenroth, C., Zhang, Y., 2010. Ribosome biogenesis surveillance: probing the ribosomal protein-Mdm2-p53 pathway. Oncogene 29, 4253–4260. https://doi.org/10.1038/onc.2010.189.

Deisenroth, C., Franklin, D.A., Zhang, Y., 2016. The evolution of the ribosomal protein–MDM2–p53 pathway. Cold Spring Harb. Perspect. Med. 6, a026138. https://doi.org/10.1101/cshperspect.a026138.

Dragon, F., Gallagher, J.E.G., Compagnone-Post, P.A., Mitchell, B.M., Porwancher, K.A., Wehner, K.A., Wormsley, S., Settlage, R.E., Shabanowitz, J., Osheim, Y., Beyer, A.L., Hunt, D.F., Baserga, S.J., 2002. A large nucleolar U3 ribonucleoprotein required for 18S ribosomal RNA biogenesis. Nature 417, 967–970. https://doi.org/10.1038/nature00769.

Drygin, D., Rice, W.G., Grummt, I., 2010. The RNA polymerase I transcription machinery: an emerging target for the treatment of cancer. Annu. Rev. Pharmacol. Toxicol. 50, 131–156. https://doi.org/10.1146/annurev.pharmtox.010909.105844.

Fernandez-Gonzalez, A., La Spada, A.R., Treadaway, J., Higdon, J.C., Harris, B.S., Sidman, R.L., Morgan, J.I., Zuo, J., 2002. Purkinje cell degeneration (pcd) phenotypes caused by mutations in the axotomy-induced gene, Nna1. Science 295, 1904–1906. https://doi.org/10.1126/science.1068912.

Garcia-Esparcia, P., Sideris-Lampretsas, G., Hernandez-Ortega, K., Grau-Rivera, O., Sklaviadis, T., Gelpi, E., Ferrer, I., 2017. Altered mechanisms of protein synthesis in frontal cortex in Alzheimer disease and a mouse model. Am. J. Neurodegener. Dis. 6, 15–25.

Gilmore-Hall, S., Kuo, J., Ward, J.M., Zahra, R., Morrison, R.S., Perkins, G., La Spada, A.R., 2018. CCP1 promotes mitochondrial fusion and motility to prevent Purkinje cell neuron loss in pcd mice. J. Cell Biol., jcb.201709028. https://doi.org/10.1083/jcb.201709028.

Ginisty, H., Amalric, F., Bouvet, P., 1998. Nucleolin functions in the first step of ribosomal RNA processing. EMBO J. 17, 1476–1486. https://doi.org/10.1093/emboj/17.5.1476.

Ginisty, H., Sicard, H., Roger, B., Bouvet, P., 1999. Structure and functions of nucleolin. J.

Cell Sci. 112 (Pt 6), 761–772.
Ginisty, H., Serin, G., Ghisolfi-Nieto, L., Roger, B., Libante, V., Amalric, F., Bouvet, P., 2000. Interaction of nucleolin with an evolutionarily conserved pre-ribosomal RNA sequence is required for the assembly of the primary processing complex. J. Biol. Chem. 275, 18845–18850. https://doi.org/10.1074/jbc.M002350200.
Greer, C.A., Shepherd, G.M., 1982. Mitral cell degeneration and sensory function in the neurological mutant mouse Purkinje cell degeneration (PCD). Brain Res. 235, 156–161.
Haeusler, A.R., Donnelly, C.J., Periz, G., Simko, E.A.J., Shaw, P.G., Kim, M.-S., Maragakis, N.J., Troncoso, J.C., Pandey, A., Sattler, R., Rothstein, J.D., Wang, J., 2014. C9orf72 nucleotide repeat structures initiate molecular cascades of disease. Nature 507, 195–200. https://doi.org/10.1038/nature13124.
Hein, N., Hannan, K.M., George, A.J., Sanij, E., Hannan, R.D., 2013. The nucleolus: an emerging target for cancer therapy. Trends Mol. Med. 19, 643–654. https://doi.org/10.1016/j.molmed.2013.07.005.
Hernández-Ortega, K., Garcia-Esparcia, P., Gil, L., Lucas, J.J., Ferrer, I., 2016. Altered machinery of protein synthesis in Alzheimer's: from the nucleolus to the ribosome. Brain Pathol. 26, 593–605. https://doi.org/10.1111/bpa.12335.
Hetman, M., Pietrzak, M., 2012. Emerging roles of the neuronal nucleolus. Trends Neurosci. 35, 305–314. https://doi.org/10.1016/j.tins.2012.01.002.
Hua, Y., Zhou, J., 2004. Survival motor neuron protein facilitates assembly of stress granules. FEBS Lett. 572, 69–74. https://doi.org/10.1016/j.febslet.2004.07.010.
Jin, J., Li, G.J., Davis, J., Zhu, D., Wang, Y., Pan, C., Zhang, J., 2007. Identification of novel proteins associated with both alpha-synuclein and DJ-1. Mol. Cell. Proteomics 6, 845–859. https://doi.org/10.1074/mcp.M600182-MCP200.
Kalinina, E., Biswas, R., Berezniuk, I., Hermoso, A., Aviles, F.X., Fricker, L.D., 2007. A novel subfamily of mouse cytosolic carboxypeptidases. FASEB J. 21, 836–850. https://doi.org/10.1096/fj.06-7329com.
Kalita, K., Makonchuk, D., Gomes, C., Zheng, J.-J., Hetman, M., 2008. Inhibition of nucleolar transcription as a trigger for neuronal apoptosis. J. Neurochem. 105, 2286–2299. https://doi.org/10.1111/j.1471-4159.2008.05316.x.
Kiss-László, Z., Henry, Y., Bachellerie, J.P., Caizergues-Ferrer, M., Kiss, T., 1996. Site-specific ribose methylation of preribosomal RNA: a novel function for small nucleolar RNAs. Cell 85, 1077–1088.
Kitano, S., Kino, Y., Yamamoto, Y., Takitani, M., Miyoshi, J., Ishida, T., Saito, Y., Arima, K., Satoh, J.-I., 2015. Bioinformatics data mining approach suggests coexpression of AGTPBP1 with an ALS-linked gene C9orf72. J. Central. Nerv. Syst. Dis. 7, 15–26. https://doi.org/10.4137/JCNSD.S24317.
Kobayashi, J., Fujimoto, H., Sato, J., Hayashi, I., Burma, S., Matsuura, S., Chen, D.J., Komatsu, K., 2012. Nucleolin participates in DNA double-strand break-induced damage response through MDC1-dependent pathway. PLoS One 7, e49245. https://doi.org/10.1371/journal.pone.0049245.
Kreiner, G., Bierhoff, H., Armentano, M., Rodriguez-Parkitna, J., Sowodniok, K., Naranjo, J.R., Bonfanti, L., Liss, B., Schütz, G., Grummt, I., Parlato, R., 2013. A neuroprotective phase precedes striatal degeneration upon nucleolar stress. Cell Death Differ. 20, 1455–1464. https://doi.org/10.1038/cdd.2013.66.
Kwak, Y.-D., Ma, T., Diao, S., Zhang, X., Chen, Y., Hsu, J., Lipton, S.A., Masliah, E., Xu, H., Liao, F.-F., 2010. NO signaling and S-nitrosylation regulate PTEN inhibition in neurodegeneration. Mol. Neurodegener. 5, 49. https://doi.org/10.1186/1750-1326-5-49.
Lachyankar, M.B., Sultana, N., Schonhoff, C.M., Mitra, P., Poluha, W., Lambert, S., Quesenberry, P.J., Litofsky, N.S., Recht, L.D., Nabi, R., Miller, S.J., Ohta, S., Neel, B.G., Ross, A.H., 2000. A role for nuclear PTEN in neuronal differentiation. J. Neurosci. 20, 1404–1413.
Lam, Y.W., Trinkle-Mulcahy, L., 2015. New insights into nucleolar structure and function. F1000Prime Rep. 7, 48. https://doi.org/10.12703/P7-48.
Lamond, A.I., Spector, D.L., 2003. Nuclear speckles: a model for nuclear organelles. Nat. Rev. Mol. Cell Biol. 4, 605–612. https://doi.org/10.1038/nrm1172.
Liang, H., Chen, X., Yin, Q., Ruan, D., Zhao, X., Zhang, C., McNutt, M.A., Yin, Y., 2017. PTENβ is an alternatively translated isoform of PTEN that regulates rDNA transcription. Nat. Commun. 8, 14771. https://doi.org/10.1038/ncomms14771.
Lim, J., Hao, T., Shaw, C., Patel, A.J., Szabó, G., Rual, J.-F., Fisk, C.J., Li, N., Smolyar, A., Hill, D.E., Barabási, A.-L., Vidal, M., Zoghbi, H.Y., 2006. A protein–protein interaction network for human inherited ataxias and disorders of purkinje cell degeneration. Cell 125, 801–814. https://doi.org/10.1016/j.cell.2006.03.032.
Matthews, D.A., 2001. Adenovirus protein V induces redistribution of nucleolin and B23 from nucleolus to cytoplasm. J. Virol. 75, 1031–1038. https://doi.org/10.1128/JVI.75.2.1031-1038.2001.
Mattson, M.P., Magnus, T., 2006. Ageing and neuronal vulnerability. Nat. Rev. Neurosci. 7, 278–294. https://doi.org/10.1038/nrn1886.
Muñoz-Castañeda, R., Díaz, D., Peris, L., Andrieux, A., Bosc, C., Muñoz-Castañeda, J.M., Janke, C., Alonso, J.R., Moutin, M.-J., Weruaga, E., 2018. Cytoskeleton stability is essential for the integrity of the cerebellum and its motor- and affective-related behaviors. Sci. Rep. 8, 3072. https://doi.org/10.1038/s41598-018-21470-2.
Ogawa, L.M., Baserga, S.J., 2017. Crosstalk between the nucleolus and the DNA damage response. Mol. BioSyst. 13, 443–455. https://doi.org/10.1039/c6mb00740f.
O'Gorman, S., Sidman, R.L., 1985. Degeneration of thalamic neurons in ? Purkinje cell degeneration? mutant mice. I. Distribution of neuron loss. J. Comp. Neurol. 234, 277–297. https://doi.org/10.1002/cne.902340302.
O'Rourke, J.G., Bogdanik, L., Muhammad, A.K.M.G., Gendron, T.F., Kim, K.J., Austin, A., Cady, J., Liu, E.Y., Zarrow, J., Grant, S., Ho, R., Bell, S., Carmona, S., Simpkinson, M., Lall, D., Wu, K., Daughrity, L., Dickson, D.W., Harms, M.B., Petrucelli, L., Lee, E.B., Lutz, C.M., Baloh, R.H., 2015. C9orf72 BAC transgenic mice display typical pathologic features of ALS/FTD. Neuron 88, 892–901. https://doi.org/10.1016/j.neuron.2015.10.027.
Parlato, R., Kreiner, G., 2013. Nucleolar activity in neurodegenerative diseases: a missing piece of the puzzle? J. Mol. Med. (Berl.) 91, 541–547. https://doi.org/10.1007/s00109-012-0981-1.
Parlato, R., Kreiner, G., Erdmann, G., Rieker, C., Stotz, S., Savenkova, E., Berger, S., Grummt, I., Schütz, G., 2008. Activation of an endogenous suicide response after perturbation of rRNA synthesis leads to neurodegeneration in mice. J. Neurosci. 28, 12759–12764. https://doi.org/10.1523/JNEUROSCI.2439-08.2008.
Perlaky, L., Valdez, B.C., Busch, H., 1997. Effects of cytotoxic drugs on translocation of nucleolar RNA helicase RH-II/Gu. Exp. Cell Res. 235, 413–420. https://doi.org/10.1006/excr.1997.3686.
Raška, I., Shaw, P.J., Cmarko, D., 2006. New insights into nucleolar architecture and activity. Int. Rev. Cytol. 177–235. https://doi.org/10.1016/S0074-7696(06)55004-1.
Rieker, C., Engblom, D., Kreiner, G., Domanskyi, A., Schober, A., Stotz, S., Neumann, M., Yuan, X., Grummt, I., Schütz, G., Parlato, R., 2011. Nucleolar disruption in dopaminergic neurons leads to oxidative damage and parkinsonism through repression of mammalian target of rapamycin signaling. J. Neurosci. 31, 453–460. https://doi.org/10.1523/JNEUROSCI.0590-10.2011.
Schmidt-Zachmann, M.S., Nigg, E.A., 1993. Protein localization to the nucleolus: a search for targeting domains in nucleolin. J. Cell Sci. 105 (Pt 3), 799–806.
Shashi, V., Magiera, M.M., Klein, D., Zaki, M., Schoch, K., Rudnik-Schöneborn, S., Norman, A., Lopes Abath Neto, O., Dusl, M., Yuan, X., Bartesaghi, L., De Marco, P., Alfares, A.A., Marom, R., Arold, S.T., Guzmán-Vega, F.J., Pena, L.D., Smith, E.C., Steinlin, M., Babiker, M.O., Mohassel, P., Foley, A.R., Donkervoort, S., Kaur, R., Ghosh, P.S., Stanley, V., Musaev, D., Nava, C., Mignot, C., Keren, B., Scala, M., Tassano, E., Picco, P., Doneda, P., Fiorillo, C., Issa, M.Y., Alassiri, A., Alahmad, A., Gerard, A., Liu, P., Yang, Y., Ertl-Wagner, B., Kranz, P.G., Wentzensen, I.M., Stucka, R., Stong, N., Allen, A.S., Goldstein, D.B., Schoser, B., Rösler, K.M., Alfadhel, M., Capra, V., Chrast, R., Strom, T.M., Kamsteeg, E., Bönnemann, C.G., Gleeson, J.G., Martini, R., Janke, C., Senderek, J., Senderek, J., 2018. Loss of tubulin deglutamylase CCP1 causes infantile-onset neurodegeneration. EMBO J., e100540. https://doi.org/10.15252/embj.2018100540.
Shen, W.H., Balajee, A.S., Wang, J., Wu, H., Eng, C., Pandolfi, P.P., Yin, Y., 2007. Essential role for nuclear PTEN in maintaining chromosomal integrity. Cell 128, 157–170. https://doi.org/10.1016/j.cell.2006.11.042.
Song, M.S., Salmena, L., Pandolfi, P.P., 2012. The functions and regulation of the PTEN tumour suppressor. Nat. Rev. Mol. Cell Biol. 13, 283–296. https://doi.org/10.1038/nrm3330.
Taha, M.S., Nouri, K., Milroy, L.G., Moll, J.M., Herrmann, C., Brunsveld, L., Piekorz, R.P., Ahmadian, M.R., 2014. Subcellular fractionation and localization studies reveal a direct interaction of the fragile X mental retardation protein (FMRP) with nucleolin. PLoS One 9, e91465. https://doi.org/10.1371/journal.pone.0091465.
Tapia, O., Narcís, J.O., Riancho, J., Tarabal, O., Piedrafita, L., Calderó, J., Berciano, M.T., Lafarga, M., 2017. Cellular bases of the RNA metabolism dysfunction in motor neurons of a murine model of spinal muscular atrophy: role of Cajal bodies and the nucleolus. Neurobiol. Dis. 108, 83–99. https://doi.org/10.1016/j.nbd.2017.08.004.
Tiku, V., Antebi, A., 2018. Nucleolar function in lifespan regulation. Trends Cell Biol. 28, 662–672. https://doi.org/10.1016/j.tcb.2018.03.007.
Tsoi, H., Lau, T.C.-K., Tsang, S.-Y., Lau, K.-F., Chan, H.Y.E., 2012. CAG expansion induces nucleolar stress in polyglutamine diseases. Proc. Natl. Acad. Sci. 109, 13428–13433. https://doi.org/10.1073/pnas.1204089109.
Valero, J., Berciano, M.T., Weruaga, E., Lafarga, M., Alonso, J.R., 2006. Pre-neurodegeneration of mitral cells in the pcd mutant mouse is associated with DNA damage, transcriptional repression, and reorganization of nuclear speckles and Cajal bodies. Mol. Cell. Neurosci. 33, 283–295. https://doi.org/10.1016/j.mcn.2006.08.002.
Wang, T., Morgan, J.I., 2007. The Purkinje cell degeneration (pcd) mouse: an unexpected molecular link between neuronal degeneration and regeneration. Brain Res. 1140, 26–40. https://doi.org/10.1016/j.brainres.2006.07.065.
Wolozin, B., 2012. Regulated protein aggregation: stress granules and neurodegeneration. Mol. Neurodegener. 7, 56. https://doi.org/10.1186/1750-1326-7-56.
Yang, C., Maiguel, D.A., Carrier, F., 2002. Identification of nucleolin and nucleophosmin as genotoxic stress-responsive RNA-binding proteins. Nucleic Acids Res. 30, 2251–2260.
Zhang, C., Comai, L., Johnson, D.L., 2005. PTEN represses RNA polymerase I transcription by disrupting the SL1 complex. Mol. Cell. Biol. 25, 6899–6911. https://doi.org/10.1128/MCB.25.16.6899-6911.2005.
Zhang, Q., Chen, Z.S., An, Y., Liu, H., Hou, Y., Li, W., Lau, K.-F., Koon, A.C., Ngo, J.C.K., Chan, H.Y.E., 2018. A peptidylic inhibitor for neutralizing expanded CAG RNA-induced nucleolar stress in polyglutamine diseases. RNA 24, 486–498. https://doi.org/10.1261/rna.062703.117.
Zhou, L., Hossain, M.I., Yamazaki, M., Abe, M., Natsume, R., Konno, K., Kageyama, S., Komatsu, M., Watanabe, M., Sakimura, K., Takebayashi, H., 2018. Deletion of exons encoding carboxypeptidase domain of Nna1 results in Purkinje cell degeneration (*pcd*) phenotype. J. Neurochem. https://doi.org/10.1111/jnc.14591.